International Journal of Pharmaceutics 374 (2009) 125–138

Contents lists available at ScienceDirect

International Journal of Pharmaceutics

journal homepage: www.elsevier.com/locate/ijpharm

Pharmaceutical Nanotechnology

Effect of homobifunctional crosslinkers on nucleic acids delivery ability of PEI nanoparticles

Archana Swami[a], Ritu Goyal[a], Sushil Kumar Tripathi[a], Naresh Singh[a], Neeraj Katiyar[b], Anil K. Mishra[b], K.C. Gupta[a,*]

[a] Institute of Genomics and Integrative Biology (CSIR), Delhi University Campus, Mall Road, Delhi 110007, India
[b] Institute of Nuclear Medicine and Allied Sciences, Lucknow Road, Delhi 110007, India

ARTICLE INFO

Article history:
Received 15 November 2008
Received in revised form 5 March 2009
Accepted 6 March 2009
Available online 19 March 2009

Keywords:
PEI nanoparticles
Gene delivery
siRNA
Cytotoxicity
Intracellular trafficking
Body distribution

ABSTRACT

Polyethylenimine (PEI), a widely used cationic polymeric vector with high transfection efficiency, was converted into nanoparticles by introducing ionic and covalent crosslinkers with varying proportion of 1,6-hexanebisphosphate (HP), adipic acid (AA) and 1,4-butane dialdehyde (BA) to obtain a small library of HP-PEI (HPP), AA-PEI (AAP) and BA-PEI (BAP) nanoparticles, respectively. Particles were characterized by spectroscopic technique as well as physicochemical parameters such as size, morphology, surface charge, effect of crosslinking on buffering capacity and DNA binding ability. The entire series of nanoparticles were compared for their cytoxicity and ability to deliver genes in various cell lines. Among various nanoparticles, AAP-3 nanoparticle/DNA complex exhibited higher transfection efficiency (1.5–7.8 folds) than the native PEI (25 kDa) and commercially available transfection reagents, such as GenePorter™, GenePorter2™, Fugene™ and Superfect™, with cell viability >85%. The highest cell viability was observed with BAP nanoparticles (>95%). Importantly, the transfection activity of nanoparticle/DNA complexes was preserved in the presence of serum. Transfection with GFP-siRNA inhibited expression of transfected GFP gene by ~81–92%. All nanoparticle types (HPP, AAP and BAP) required a comparable time for entry into cells and subsequent intracellular passage from the cytoplasm to the nucleus. Intravenous delivery of ^{99}Tc labeled BAP-2/DNA complex to female Balb/c mice revealed the presence of the complex in most of the organs with the highest retention in liver. In conclusion, HPP, AAP and BAP nanoparticles are safe for efficient gene delivery.

1. Introduction

Nucleic acids have tremendous potential as therapeutics for the treatment of genetic disorders and infectious diseases (Olefsky, 2000; Rosenecker et al., 2006; Edelstein, 2007; Nienhuis, 2008; Seth, 2008; Vinge et al., 2008; Pirollo and Chang, 2008). However, a successful delivery of nucleic acids to the targeted tissues or cells depends on the efficiency of the carrier with optimal stability in biological milieu (Davis, 1997). Among viral and non-viral vectors, the former exhibit high transfection efficiency and long-term gene expression, but their therapeutic applications have been stalled by severe immunogenicity and cytotoxicity (Zhang and Godbey, 2006). Therefore, synthetic non-viral vectors are being considered as efficient alternatives as these vectors can be produced on large-scale, lack specific immune response, have high cargo capacity and can have potential cell targeting property (Niidome and Huang, 2002; Schmidt-Wolf and Schmidt-Wolf, 2003).

Cationic polymers, e.g. polyethylenimine (PEI), poly(L-lysine) (PLL), polyallylamine (PAA), chitosan, dendrimers based on polyamindoamine (PAMAM) and liposomes have emerged as promising materials for intracellular delivery of nucleic acids (Guang Liu and De Yao, 2002; Itaka et al., 2003; Tabatt et al., 2004; Kono et al., 2005; Pathak et al., 2007; Malek et al., 2008). Of these, PEI is studied extensively due to its high cationic charge density that allows effective condensation of nucleic acids and its protection from degradation (Fischer et al., 2003). Moreover, the in-built endosomolytic activity of PEI by the 'proton sponge' effect allows complexed nucleic acid to escape from endosome (Sonawane et al., 2003). Besides, PEI also directs DNA into the nucleus (Godbey et al., 1999). The high charge density of PEI contributes significantly towards cytotoxicity due to interaction with negatively charged cellular membranes (Jeong et al., 2006; Hong et al., 2006). In order to reduce the charge associated cytotoxicity of PEI, several groups have modified PEI by partially masking its charge, following tedious synthetic routes (Diebold et al., 1999; Gosselin et al., 2001; Petersen et al., 2002; Patnaik et al., 2006; Nimesh et al., 2006a, 2007). Introduction of certain degree of hydrophobicity into the system also enhances PEI's binding affinity to cell membrane and ability to penetrate cells (SanJuan et al., 2007).

* Corresponding author. Tel.: +91 11 27662491; fax: +91 11 27667471.
E-mail address: kcgupta@igib.res.in (K.C. Gupta).

0378-5173/$ – see front matter © 2009 Elsevier B.V. All rights reserved.
doi:10.1016/j.ijpharm.2009.03.009

Recently, we (Nimesh et al., 2006a; Swami et al., 2007a,b) have prepared PEI nanoparticles that were crosslinked electrostatically and covalently and evaluated these for transfection efficiency and cell viability. The high transfection efficiency and reduced cytotoxicity of the resulting nanoparticle systems prompted us to investigate the effect of linkers with different functional groups on their efficacy in delivering nucleic acids to cells when used to modify PEI. Here, we have prepared a small library of PEI nanoparticles from three homobifunctional crosslinkers, 1,6-hexanediol bisphosphate (HP), adipic acid (AA) and 1,4-butane dialdehyde (BA), without altering the C-6 linker length and assessed the resulting nanoparticles (HPP, AAP and BAP) for DNA binding, *in vitro* transfection efficiency (both in presence and absence of serum) and cytotoxicity in different cell lines. These nanoparticles were characterized for size, morphology and surface charge. *In vitro* transfection efficiency of these nanoparticles was compared with unmodified PEI (25 kDa), GenePorter™, GenePorter2™, Fugene™ and Superfect™. Organ distribution studies of BAP-2/DNA complex, after i.v. administration in Balb/C mice, was also carried out, which revealed the highest retention of the complex in the liver even 24 h post-administration.

2. Materials and methods

2.1. Cell culture and materials

HEK293, HeLa and A549 cells were obtained from NCCS, Pune, India. Cell cultures were maintained (37 °C, 5% CO_2—air) in Dulbecco's Modified Eagle's Culture Medium (DMEM) (Sigma, USA) supplemented with 10% heat-inactivated fetal calf serum (GIBCO-BRL-Life Technologies, UK) and 1% antibiotic cocktail of streptomycin and penicillin.

Specialized chemicals and reagents, used in the present study, were procured from their respective suppliers such as branched PEI (Mw 25 kDa), polyethyleneglycol (Mw 4000 Da), MTT kit, hexane-1,6-diol, adipic acid, 1-ethyl-3-(3-dimethylaminopropyl) carbodiimide (EDAC), fluorescein isothiocyanate (FITC), sodium cyanoborohydride and high retention dialysis tubing (Sigma–Aldrich Chemical Co., USA), Bradford reagent (Bio-Rad Inc., USA), transfection agents such as Superfect™ (Qiagen, France), Fugene™ (Roche Applied Science, USA), and GenePorter™ and GenePorter2™ (Gelantis, USA), plasmid purification kit (Qiagen, France) and the plasmid pEGFPN3 (Clontech, USA). Sodium pertechnetate eluted fresh from ^{99m}Mo by solvent extraction method (Garg et al., 2008) was procured from Regional Centre for Radiopharmaceuticals (Department of Atomic Energy, India). Balb C mice (2–3 month-old, 25–30 g wt) were used for *in vivo* studies. Other fine chemicals of the highest grade were stannous chloride (extrapure Ph Eur., BP grade, Merck, Germany) and chromatography grade acetone and aldehyde free 100% acetic acid (Merck, India). FTIR spectra of nanoparticles were recorded on a single beam PerkinElmer (Spectrum BX Series), USA. Particle size and zeta potential were determined on Zetasizer Nano-ZS (Malvern Instruments, UK). Particle size was also measured by atomic force microscopy (PicoSPM System, Molecular Imaging, USA). Green fluorescent protein (GFP) in transfected cells was assayed (excitation at 488 nm, emission at 509 nm) on NanoDrop™ ND-3300 spectrofluorometer (USA). The uptake and intracellular passage of fluorescein labeled nanoparticles/DNA complexes were monitored in LSM 510 Meta Zeiss, Germany).

2.2. Synthesis

2.2.1. Synthesis of siRNA

The following oligonucleotide sequences were synthesized following phosphoramidite chemistry and purified on RP-HPLC:

T7 primer: d (TAA TAC GAC TCA CTA TAG)

GFP sense: d (ATG AAC TTC AGG GTC AGC TTG CTA TAG TGA GTC GTA TTA)

GFP antisense: d (CGG CAA GCT GAC CCT GAA GTT CTA TAG TGA GTC GTA TTA)

After annealing T7 primer sequence to GFP sense or antisense oligonucleotides, complementary strands were synthesized by T7 RNA polymerase (Milligan and Uhlenbeck, 1989). The sense and antisense RNA strands were annealed and double stranded siRNA was used for transfection.

2.2.2. Synthesis of hexane-1,6-diol bisphosphate (HP)

Hexane-1,6-diol bisphosphate was synthesized from 1,6-hexanediol and phosphorous oxychloride. To a 50 ml round bottom flask, 1,6-hexanediol (1 g, 8.46 mmol) was mixed with 20 ml of dry pyridine and co-evaporated twice on a rotary evaporator, resuspended in 15 ml of dry chloroform and added to a solution of phosphorous oxychloride (4.65 ml, 50.76 mmol, mixed with 25 ml of dry chloroform) drop-wise over a period of 30 min. The reaction mixture was refluxed for 3 h followed by removal of chloroform and excess phosphorous oxychloride under vacuum. The resultant viscous solid was hydrolyzed by drop-wise addition of distilled water (50 ml) over a period of 20 min and the solution was further refluxed for 5 h and concentrated on a rotary evaporator. The residue was dissolved in 50 ml methanol followed by the addition of ether till turbidity appeared and kept at −20 °C for 24 h. The sticky residue was separated and dried in a desiccator under vacuum, weighed (yield = 85%) and characterized by its IR. IR (KBr) cm^{-1}: 2942, 2866, 1446, 1280, 1030 (P–O–C stretching), 728.

2.2.3. Synthesis of 1,4-butane dialdehyde (BA)

In a 250 ml round bottom flask, hexane-1,6-diol (250 mg, 2.1 mmol) was taken up in ethyl acetate (75 ml) and added o-iodoxybenzoic acid (IBX, 3.55 g, 12.6 mmol) (More and Finney, 2002). The resulting suspension was stirred vigorously at 80 °C in an oil bath. After 4 h (completion of the reaction monitored on tlc), it was allowed to cool to room temperature and filtered through a Buchner funnel. The residue was washed with ethyl acetate (3× 20 ml) and the combined filtrates were concentrated on a rotary evaporator to obtain 1,4-butane dialdehyde in ∼92% yield, as a syrupy material, which was characterized by its ^{1}H NMR and IR. ^{1}H NMR ($CDCl_3$) δ: 1.2–1.6 (m, 4H), 2.3–2.5 (m, 4 H), 9.6 (t, 2H). IR (KBr) cm^{-1}: 3423, 2953, 1723, 1115.

2.3. Preparation of nanoparticles

2.3.1. Preparation of hexane-1,6-diol bisphosphate-PEI (HPP) nanoparticles

To a solution of PEI (50 mg dissolved in 50 ml H_2O), a 50% methanolic solution of hexane-1,6-diol bisphosphate (6.25 mg/6.25 ml, for 4% crosslinking) was added drop-wise over a period of 15 min with vigorous stirring. After 4 h, the solution was dialysed (using 12 kDa cut off membrane) against deionised water for 48 h with intermittent change of water (4 times). The solution was lyophilized to obtain HPP nanoparticles in ∼88% yield and characterized by its IR. IR (KBr) cm^{-1}: 3402 (NH stretching), 1475, 988 (P–O–C stretching).

HPP nanoparticles with 8%, 12%, and 16% crosslinking were also prepared by varying hexane-1,6-diol bisphosphate content and characterized.

2.3.2. Preparation of adipic acid-PEI (AAP) nanoparticles

AAP nanoparticles were prepared as described above except a 50% methanolic solution of adipic acid (3.4 mg/3.4 ml, for 4% crosslinking) was used, followed by the addition of EDAC (10 mg).

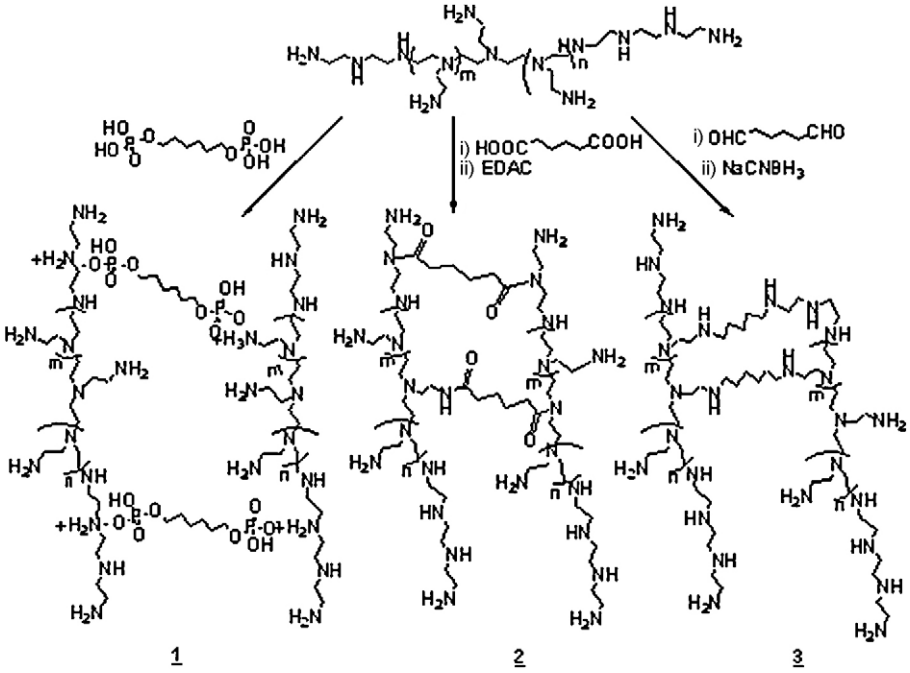

Scheme 1. Scematic representation of the preparation of (1) HPP, (2) AAP and (3) BAP nanoparticles.

The resulting solution was allowed to stir at room temperature for 24 h, then subjected to dialysis, as described above and lyophilized to obtain nanoparticles in ~80% yield, which were then characterized by IR spectroscopy. IR (KBr) cm^{-1}: 3272 (NH stretching), 1646 (CO stretching), 1567 (NH_2 scissoring), 1556 (NH-amide band), 1113 (CN stretching), 816 (NH_2 and NH wagging).

Similarly, a series of AAP nanoparticles with different crosslinking (8%, 12% and 16%) were prepared and characterized.

2.3.3. Preparation of 1,4-butane dialdehyde (BAP) nanoparticles

To a solution of PEI (50 mg in 50 ml H_2O), a 50% methanolic solution of 1,4-butane dialdehyde (2.7 mg/2.7 ml, for 4% crosslinking) was added drop-wise during 15 min with vigorous stirring at room temperature. After 4 h, sodium cyanoborohydride (15 mg) was added, the reactants allowed to stir overnight and processed, as described above to get BAP nanoparticles in ~85% yield followed by their characterization by IR spectroscopy. IR (KBr) cm^{-1}: 3363 (N–H stretching), 2954 (C–H stretching), 1568 (NH_2 scissoring), 1068 (C–N stretching), 817 (NH_2 and N–H wagging).

Likewise, BAP nanoparticles with different crosslinking (8%, 12% and 16%) were obtained and characterized.

The extent of crosslinking in all the three series of nanoparticles was determined through quantification of the free amino groups following 2,4,6-trinitrobenzenesulfonic acid (TNBS) method (Tseng et al., 2004).

2.4. Formation of nanoparticle/DNA complexes

To form nanoparticle/DNA complexes, an aqueous solution of HPP nanoparticles (1 mg/ml) was added to 1 μl of DNA (0.3 μg/μl) at various weight ratios (0.5:1, 1:1, 1.5:1, 2:1) and the final volume was made up to 20 μl with water. For *in vitro* transfection assay, 5 μl dextrose (20%) was added before making up the final volume to 20 μl with water. The resulting samples were gently vortexed and incubated for 30 min (room temperature) prior to their use in biophysical studies or transfection experiments. Similarly, AAP and BAP nanoparticles/DNA complexes were prepared and used.

2.5. Physical characterization of nanoparticles

The nanoparticles, prepared in the present study, were characterized for morphology, size and zeta potential. The hydrodynamic diameter of nanoparticles (1 mg/ml) and their DNA complexes, suspended in water and 10% serum, were measured by DLS in triplicates using Zetasizer Nano ZS. The data analysis was performed in automatic mode and measured sizes were presented as the average value of 20 runs (Swami et al., 2007a).

To characterize the morphology of nanoparticles and their DNA complexes, a suspension of nanoparticles (2–3 μl, 0.1 μg/ml) was deposited on a freshly split untreated mica strip, dried for 5 min (room temperature) and imaged. Particle size was estimated by an image analyzing software (SPIP) for scanning probe microscopy (Swami et al., 2007a).

Zeta potential measurements of nanoparticles and DNA complexes in water and 10% serum were measured on a Zetasizer Nano ZS, carried out 30 runs in triplicates and the average values are esti-

Table 1
Percent substitution in HPP, AAP and BAP nanoparticles.

S. no.	Samples	Attemped (%) substitution	Realised (%) substitution (TNBS)
1	AAP-1	8	5.714
2	AAP-2	16	10.098
3	AAP-3	24	15.712
4	AAP-4	32	18.670
5	BAP-1	8	7.825
6	BAP-2	16	15.669
7	BAP-3	24	22.071
8	BAP-4	32	31.104
9	HPP-1	8	6.045
10	HPP-2	16	11.273
11	HPP-3	24	19.411
12	HPP-4	32	23.894

Table 2
Particle size and zeta potential measurements of HPP, AAP and BAP nanoparticles and their corresponding DNA complexes at w:w ratio of 3.33 for nanoparticle/DNA and w:w ratio of 1.7 for PEI/DNA complexes.

Samples	Average particle size in nm ± S.D.			Zeta potential in mV ± S.D.		
	Nanoparticle (in H_2O)	DNA bound nanoparticle (in H_2O)	DNA bound nanoparticle (in serum)	Nanoparticle (in H_2O)	DNA bound nanoparticle (in H_2O)	DNA bound nanoparticle (in serum)
HPP-1	203 ± 12.7	220 ± 7.9	157 ± 12.2	33.6 ± 1.2	24.3 ± 1.8	−10.1 ± 1.2
HPP-2	164 ± 11.8	186 ± 7.5	125 ± 12.4	31.1 ± 1.4	20.1 ± 1.6	−10 ± 1.1
HPP-3	130 ± 11.0	151 ± 8.1	101 ± 1.5	28.5 ± 1.2	18.8 ± 1.4	−10.1 ± 1.0
HPP-4	108 ± 10.6	133 ± 6.6	89 ± 10.3	25.8 ± 1.7	16.1 ± 1.4	−9.9 ± 1.1
AAP-1	211 ± 11.2	228 ± 8.2	162 ± 7.8	34.3 ± 1.3	24.8 ± 1.3	−9.8 ± 1.3
AAP-2	178 ± 10.4	201 ± 8.3	141 ± 7.9	31.8 ± 1.8	22.7 ± 1.3	−9.8 ± 1.1
AAP-3	148 ± 7.8	165 ± 5.7	113 ± 8.5	29.1 ± 1.5	19.2 ± 1.1	−9.6 ± 1.2
AAP-4	126 ± 7.3	144 ± 5.9	97 ± 9.7	26.4 ± 1.1	16.8 ± 2.1	−9.7 ± 0.9
BAP-1	173 ± 10.2	196 ± 7.1	142 ± 6.8	35.2 ± 1.1	25.1 ± 1.6	−9.8 ± 1.2
BAP-2	118 ± 10.4	131 ± 6.0	95 ± 7.4	33.8 ± 1.5	23.4 ± 1.8	−9.5 ± 1.2
BAP-3	90 ± 8.1	112 ± 5.2	86 ± 8.3	32.6 ± 1.4	22.1 ± 1.9	−9.4 ± 1.3
BAP-4	78 ± 6.6	101 ± 4.8	67 ± 7.0	29.9 ± 1.3	20.5 ± 1.5	−9.5 ± 1.4
PEI	–	396 ± 14.8	271 ± 12.3	41.1 ± 6.2	29.7 ± 1.3	−9.3 ± 1.3

mated by Smoluchowski approximation from the electrophoretic mobility (Swami et al., 2007b).

2.6. Buffering capacity

The ability of PEI and PEI nanoparticles to resist acidification was experimentally demonstrated by acid titration assay following a reported method (Swami et al., 2007b). A suspension of nanoparticles (HPP, AAP and BAP) (10 mg/ml) in 150 mM NaCl was adjusted to pH 12 with 0.1N NaOH and then the pH was reduced to 3.0 with 5 μl aliquots of 0.1 N HCl. pH values were recorded after each addition. The slope of the line in the plot for pH and the amount of HC1 consumed indicates the intrinsic buffering capability of the system.

2.7. DNA mobility shift assay

Branched PEI (25 kDa) was complexed with DNA (0.3 μg/μl) at w:w ratio 0.17, 0.33, 0.5 and 0.66, as described above and for nanoparticles (HPP, AAP and BAP), this ratio was 0.66, 1.33 and 2.0. DNA complexes (20 μl) were mixed with 2 μl xylene cyanol (in 20% glycerol), electrophoresed (100 V, 1 h) in 0.8% agarose, stained with ethidium bromide and visualized on a UV transilluminator using a Gel Documentation system (Bio-Rad, CA, USA) (Swami et al., 2007b).

2.8. DNA release assay

DNA (0.3 μg, 15 μg/ml) was mixed with EtBr (0.02 μg, 1 μg/ml) and the fluorescence was set to 100%. HPP, AAP and BAP nanoparticles (w:w ratio 3.33) and native PEI (w:w ratio 1.7) were added separately and the fluorescence was measured, with the background fluorescence set to zero using EtBr (1 μg/ml) alone. Heparin, a polyanion, was added in small aliquots of 2–5 U for competitive DNA displacement, to determine the relative strength of interactions between DNA and nanoparticles. The samples were incubated for 20 min after each addition and the fluorescence was

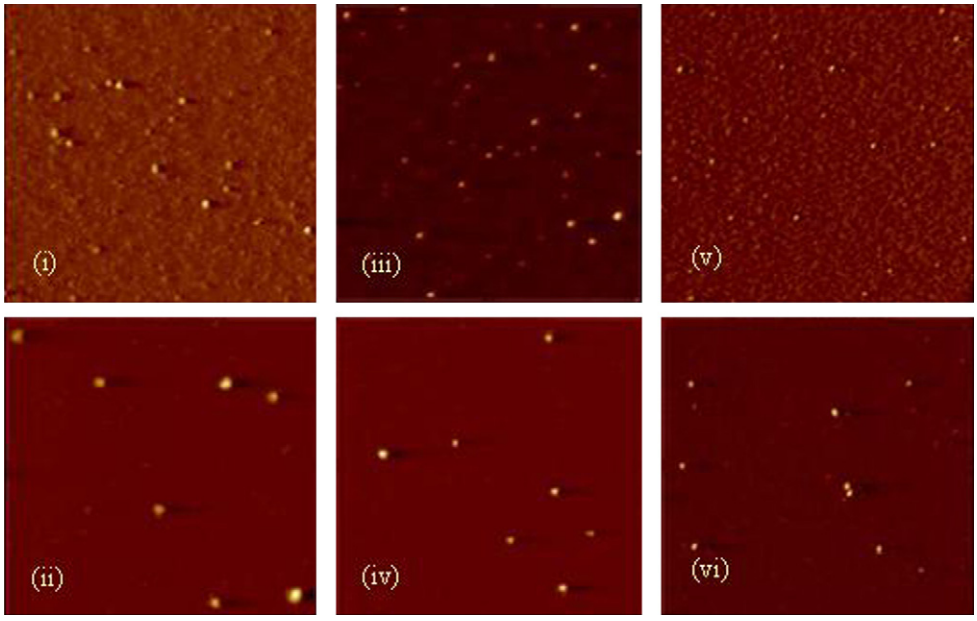

Fig. 1. Characterization of nanoparticles by atomic force microscopy. 2–3 μl of nanoparticle solution was deposited on a freshly split untreated mica strip and images were recorded in Acoustic mode. AFM image of (i) HPP-2 nanoparticle (100 nm average size); (ii) HPP-2 nanoparticle/DNA complex (110 nm average size); (iii) AAP-3 nanoparticle (90 nm average size); (iv) AAP-3 nanoparticle/DNA complex (100 nm average size); (v) BAP-2 nanoparticle (75 nm average size); (vi) BPP-2 nanoparticle/DNA complex (85 nm average size). All the images are at same magnification with an area of 3 μm × 3 μm.

measured for 1 μl aliquots of reaction mixture on NanoDrop™ ND-3300 spectrofluorometer, as before (Swami et al., 2007b).

2.9. In vitro transfection

HEK293, A549 and HeLa cells were seeded separately in 96-well plates and after 16 h, media was aspirated and cells washed with phosphate buffer saline (PBS). PEI nanoparticles (HPP, AAP and BAP) were complexed with DNA (0.3 μg) at weight ratios 1.7, 3.33, 5.0 and 6.66, and for PEI the weight ratios 0.83, 1.7 and 2.5 (Swami et al., 2007a). Similarly, DNA complexes were prepared with GenePorter™, GenePorter2™, Superfect™ and Fugene™ following manufacturer's protocol. DNA complexes were diluted with serum-free DMEM (60 μl) and gently added to HEK293, A549 and HeLa cells. In another set, DNA complexes were diluted in DMEM supplemented with 10% FCS and added to various cells. After 4 h, the transfection medium was replaced by 200 μl fresh DMEM-10% FCS and cells were incubated for 36 h.

In another experiment, 2 μl GFP-specific siRNA (2.5 μM) was added along with 1 μl of pGFP DNA (1.4 nM) to obtain nanoparticle/DNA/siRNA complex for AAP-3, BAP-2 and HPP-2 systems in a 20 μl reaction mixture and used to transfect HeLa cells. Nanoparticle/DNA complexes for HPP-2, AAP-3 and BAP-2 alone served as control. HeLa cells were also transfected with Fugene™/DNA/siRNA and Fugene™/DNA complexes. GFP expression was monitored in all experiments performed at least thrice.

2.10. Quantification of EGFP expression

EGFP expression in mammalian cells was quantitatively estimated on NanoDrop ND-3000 spectrofluorometer. After 36 h of transfection, cells were washed with PBS (2× 100 μl), lysed (10 mM Tris, 1 mM EDTA and 0.5% SDS pH 7.4, 100 μl) and agitated for 20 min at 25 °C. GFP was estimated spectroflurometrically in 2 μl lysates and corrected for background and auto-fluorescence in mock-treated cells. Total protein content in cell lysate from each well was estimated using Bradford reagent with BSA (Banglore Genei, India) as the standard. The GFP fluorescence, estimated in triplicates, expressed the fluorescence as arbitrary units/mg protein after subtracting the background.

2.11. Cytotoxicity

The cytotoxicity of HPP, AAP and BAP and nanoparticle/DNA complexes as well as Genepoter™/DNA, Genepoter2™/DNA, Superfect™/DNA and Fugene™/DNA complexes was evaluated in HEK293, A549 and HeLa cells transfected for 4 h by MTT colorimetric assay as before (Swami et al., 2007a). The relative cell viability was expressed as $[abs]_{transfected}/[abs]_{control} \times 100$. IC_{50} value or the concentration of nanoparticle/DNA complexes, at which the HEK293 cell viability reaches 50%, was estimated for our nanoparticle/DNA and PEI/DNA complexes at w:w ratio 3.33 and 1.7, respectively. The transfection efficiency for HPP, AAP and BAP nanoparticles and PEI was found to be highest at these w:w ratios.

2.12. Confocal laser scanning microscopy (CLSM)

In order to perform intracellular trafficking, nanoparticles (HPP-2, AAP-3, BAP-2) were labeled with FITC. Briefly, AAP-3 nanoparticles (10 mg in H_2O, 10 mg/ml) were conjugated with FITC (0.22 mg in DMF, 1 mg/100 μl, for 1% amines) by adding the latter to a suspension of nanoparticles and stirred overnight, concentrated in a Speed Vac and unreacted/hydrolyzed FITC was removed with ethyl acetate (3× 2 ml). In a similar manner, other nanoparticles (HPP-2 and BAP-2) were also labeled with FITC. The residual free amino groups were estimated by performing TNBS assay (Tseng et al., 2004).

HeLa cells were seeded (1.5×10^5 cells/well) on circular glass coverslips in a 6-well plate, grown overnight to 70% confluence and then incubated (37 °C) for 0.5 h, 1 h, 2 h and 4 h with a suspension of fluoresceinyl-nanoparticles (5.0 μg/ml in DMEM). Media was aspirated, cells were washed with PBS (3× 1 ml) and fixed with 4% paraformaldehyde. Nuclei were stained with DAPI and the

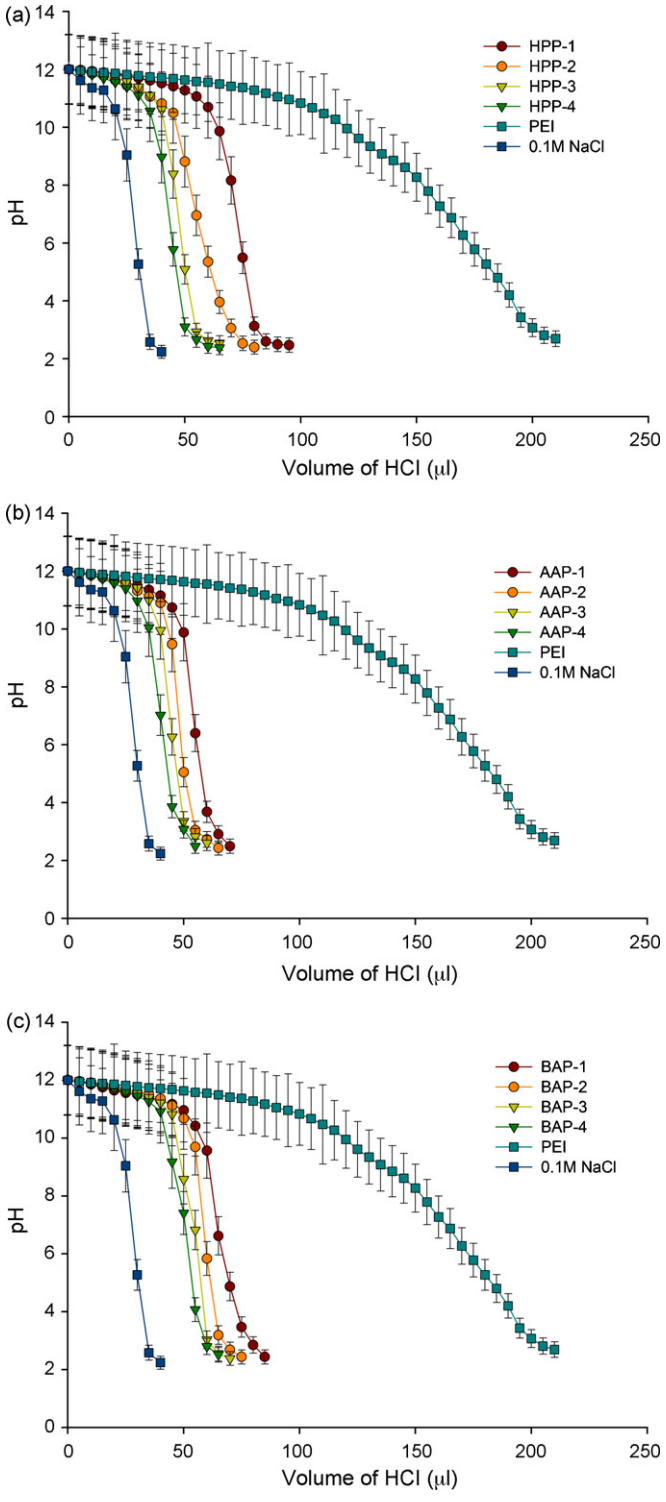

Fig. 2. Buffering capacity of PEI and nanoparticles (HPP, AAP, and BAP). Error bars represent ±standard deviation from the mean.

coverslips were mounted on glass slides with fluorescence-free Mounting Medium (UltraCruz™, Santa-Cruz Biotechnology, USA) and visualized in a confocal microscope.

2.13. DNase I protection assay

To corroborate the ability of the nanoparticles (BAP-2) to protect the condensed DNA, DNase I protection assay was performed. Native DNA and BAP-2/DNA complex (at w:w ratio 3.33) were incubated (37 °C for 15 min, 30 min, 1 h and 2 h) with 1 μl DNase I (1000 units/ml in a buffer containing 100 mM Tris, 25 mM $MgCl_2$ and 5 mM $CaCl_2$). Treatment with PBS alone served as control. After incubation, 5 μl of 100 mM EDTA was added (10 min) to inactivate DNase I and the mixture was further incubated for 2 h (room temperature) with 10 μl Heparin (5 mg/ml) to dissociate DNA complexes. Samples were electrophoresed in 0.8% agarose, stained with EtBr, visualized (Gebhart et al., 2002) and photographed on the Alpha Imager (Alpha Innotech, San Leonardo, CA). The amount of DNA released from complexes after heparin treatment was estimated by densitometry.

2.13.1. Radiolabeling of BAP-2

BAP-2/DNA complex labeled with $^{99m}TcO_4^-$ (Thakkar et al., 2004; Reddy et al., 2004a,b, 2005; Banerjee et al., 2005) was passed through Sephadex G-20 and eluted with normal saline and the radioactivity was determined with a dose calibrator (CRC 15R, Capintec Inc., USA). All fractions were observed under transmission electron microscope to confirm the purity of labeled samples, which were stored in sterile vials that were subsequently evacuated and sealed.

2.13.2. Body distribution

Distribution of BAP-2/DNA complex after i.v. injection in female mice was measured as described in the reported methods (Reddy et al., 2004a,b). Three groups (3mice/group) of animals were fasted overnight, but with free access to water. Mice were injected through the tail vein 100 μCi/100 μl of labeled complex and sacrificed after 1 h, 3 h, 6 h and 24 h. Blood was collected by cardiac puncture. Heart, lung, liver, spleen, kidney, stomach, intestine and brain were retrieved, washed with normal saline, wiped with kleenex, weighed and radioactivity measured in a γ-scintillation counter was expressed relative (%) to the injected dose.

3. Results and discussion

Gene therapy possesses a tremendous potential for the successful treatment of both inherited and acquired diseases. Several strategies for gene therapy have already been accomplished *in vitro* and *in vivo* and a few have reached clinical trials. However, a safe and efficient delivery system for nucleic acids is still elusive. In a quest to provide efficient transfer of nucleic acid to cells, we have reported PEI nanoparticle-based carriers. Here, we have prepared a small library of nanoparticles of PEI using three different homobifunctional crosslinkers bearing different functional groups that can interact, ionically and covalently, with amino groups of the cationic polymer polyethylenimine, keeping fixed the length of the alkyl chain (C-6) and examined how changed functionalities on the crosslinkers influence the transfection efficiency and cell viability of the resulting PEI nanoparticles. We selected three crosslinkers, namely, 1,6-hexanediol bisphosphate (HP), adipic acid (AA) and butan-1,6-dial (BA), keeping in mind the biocompatibility of carboxyl and phosphate functions in the cellular environment. HP interacts electrostatically with amino groups of PEI by ionic crosslinking involving primary, secondary as well as tertiary amines and AA reacts covalently with primary and secondary amino groups of PEI in the presence of EDAC, while BA forms Schiff's base selectively with primary amino groups in PEI, which are reduced subsequently to achieve covalent crosslinking via conversion of pri-

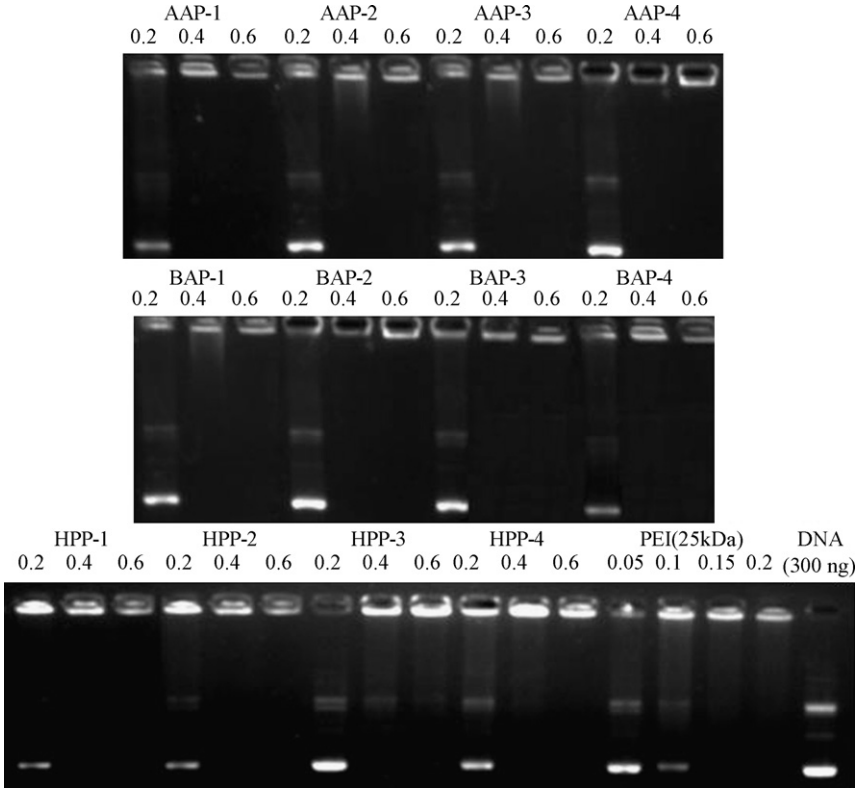

Fig. 3. DNA shift mobility assay of AAP, BAP and HPP nanoparticle/DNA and PEI/DNA complexes. pDNA (0.3 μg) was incubated with increasing amounts of nanoparticles in 5% dextrose and incubated for 20 min. Samples were electrophoresed in 0.8% agarose gel at 100 V for 45 min.

mary amines to secondary amines so that the net charge on the BAP nanoparticles remains unaltered, instead, the charge responsible for cytotoxicity (primary amines) is converted to the 'beneficial' charge of secondary amines that assist intracytoplasmic endosome rupture to release the nanoparticle/DNA complexes (Gao and Liu, 2005).

3.1. Preparation and characterization of PEI nanoparticles

PEI was crosslinked (4%, 8%, 12% and 16%) with three different crosslinkers, HP, AA and BP, to obtain three series of nanoparticles (HPP, AAP and BAP) (Scheme 1). The extent of crosslinking was controlled by adjusting the molar ratio of the crosslinkers and PEI to yield nanoparticles in 80–85% that were characterized by FTIR. The bands at 1556 (amide stretching), 1475 and 988 (P–O–C stretching) confirmed the preparation of HPP and AAP nanoparticles, respectively. The extent of primary amino groups involved in the crosslinking was determined by 2,4,6-trinitrobenzenesulfonic acid (TNBS) method (Tseng et al., 2004). The results (Table 1) showed that, for HPP and AAP nanoparticles, 58–77% of primary amino groups were involved in crosslinking, whereas, the value in BAP nanoparticles was 92–98%, as the crosslinker specifically reacts with primary amino functions of PEI.

3.2. Size, surface morphology and zeta potential measurements

Hydrodynamic diameter of the PEI nanoparticles was determined by DLS (Table 2). For HPP, AAP and BAP series, the size of the nanoparticles was found to be in the ranges 203–108 nm, 211–126 nm and 173–78 nm, respectively (Table 2), with a low polydispersity index (<0.4). Furthermore, size of the nanoparticles increased after loading DNA (Table 2), but somehow reduced in the presence of 10% FCS (Table 2). Surface morphology of the nanoparticles, assessed by AFM, revealed the spherical shape of selected nanoparticles and their DNA complexes, with low polydispersity, as shown in Fig. 1.

The surface charge (zeta potential) of the nanoparticles within a series, decreased with increasing degree of crosslinking (Table 2). Zeta potential of nanoparticles also decreased upon DNA complexing, but still had positive values. However, in 10% serum, the zeta potential of the nanoparticle/DNA complexes became negative. We noted that the zeta potential in BAP series did not decrease to the same extent as in AAP and HPP series.

The particle size distribution pattern showed low polydipersity of the nanoparticles, which did not form aggregates. The decreased size and zeta potential of nanoparticles with increasing concentration of crosslinker in the formulations is probably due to compactness of the polymer and partial charge conversion or masking. Unlike HPP and AAP series, the change in zeta potential of BAP series is small which may be attributed to the charge conversion on reaction of aldehydic groups with primary amines of PEI rather than blockage of charge as observed in the case of reaction with acid groups (carboxylic acid and phosphoric acid) (Nimesh et al., 2006b, 2007). Similar to our earlier results on 1,4-butandiol diglycidyl ether crosslinked PEI nanoparticles (Swami et al., 2007a), the size of nanoparticle/DNA complexes measured by DLS decreased in the presence of serum probably due to the loss of water to 10% serum leading to their compaction. Though crosslinking reduces the zeta potential of nanoparticles to a value lower than that of PEI (41.1 mV), it is sufficient to allow them to interact directly with the inner surface of the endosome membrane and promote its disruption, consistent with the role of charge in endosomal release of DNA complex (Walker et al., 2005).

3.3. Buffering capacity

The endosomal release of nanoparticle/DNA complexes in the cell is dependent on the proton capturing tendency of the deliv-

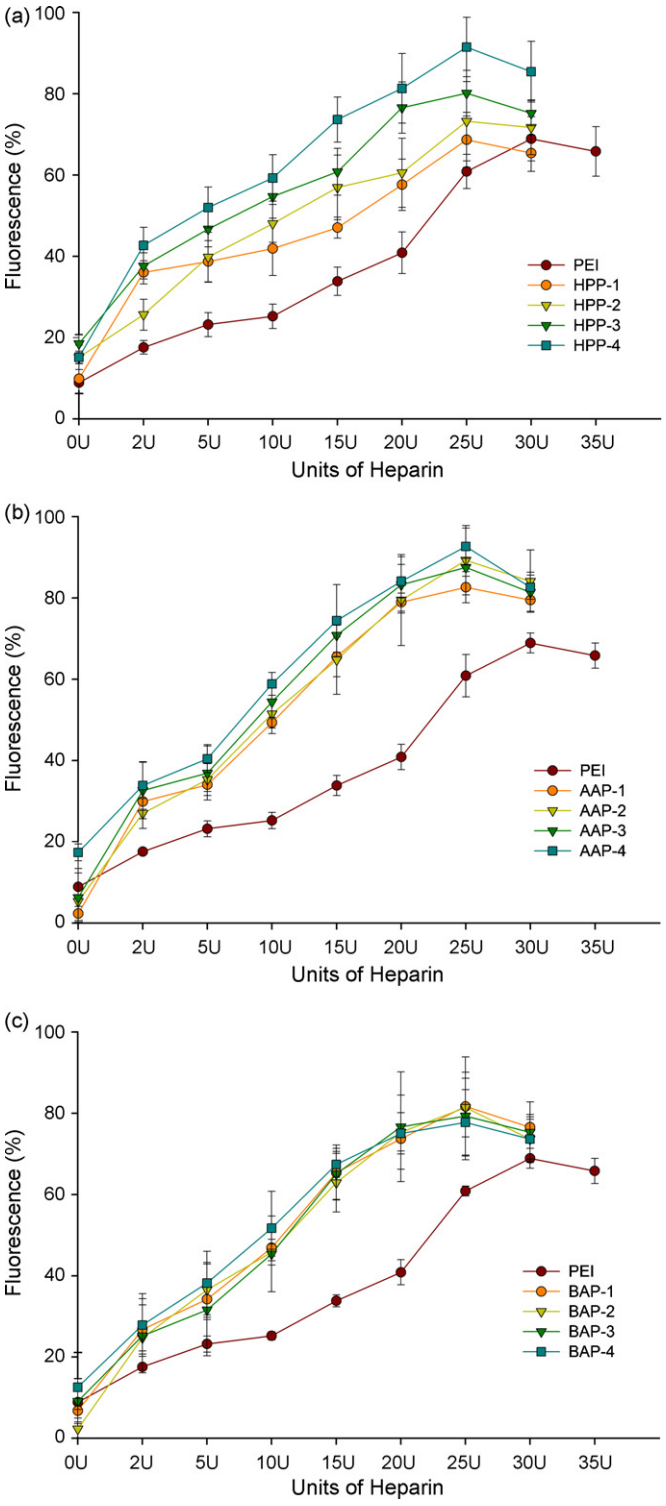

Fig. 4. DNA release assay of PEI and nanoparticles (HPP, AAP and BAP). To a 20 μl aqueous solution of ethidium bromide (1 μg/ml), 300 ng of DNA (pEGFP) (0.3 μg/μl) was added and fluorescence measured using 506 nm excitation and 610 nm emission and set to 100%. Background fluorescence was set to 0% using ethidium bromide (1 μg/ml) solution alone. To the above solution, PEI and nanoparticles were added. Subsequently, heparin, in increasing concentration, was added to the solution and fluorescence recorded. Error bars represent ±standard deviation from the mean.

ery agent (Sonawane et al., 2003). Native PEI exhibits considerable buffering capacity over a pH range 3–10 due to 'proton sponge' effect (Nimesh et al., 2007). It helps in release of DNA from endosomes/lysosomes (Akinc et al., 2005). The buffering capacity of the studied nanoparticles (HPP, AAP and BAP) was determined by an acid–base titration method (see Section 2, Fig. 2) and it was found (Fig. 2a–c) that proton capturing tendency of the nanoparticles decreased on increasing the proportion of crosslinking. This may reflect the fact that, upon crosslinking, some of the charge on PEI gets embedded inside the nanoparticles and remains unavailable for charge neutralization.

When PEI was crosslinked with BA crosslinker, primary amines were converted into secondary amines, which should have improved the buffering capacity of the resulting nanoparticles, however, a decrease in the same was observed which might be due to the fact, as described above, that some of secondary and tertiary amines get embedded inside the core of the nanoparticles and remained inaccessible for charge neutralization. This is not the case with PEI where all the amines are freely available for neutralization and thus the protonation tendency of BAP nanoparticles was found to be less than that of PEI. However, it was found that even this reduced buffering capacity of PEI nanoparticles was sufficiently enough to help in the endosomal release of the nanoparticle/DNA complexes into the cytoplasm, resulting in an excellent GFP expression.

3.4. DNA mobility shift assay

DNA binding to PEI nanoparticles was examined at different weight ratios (w:w) in DNA retardation assay (Fig. 3). Complete retardation of 0.3 μg of pDNA required 0.15 μg of native PEI, whereas, 3 times more amount (0.4 μg) of nanoparticles (HPP, AAP and BAP) was required to retard the same amount of DNA (Fig. 3). This is probably due to the higher cationic charge of PEI than nanoparticles so that the positive charge is partially blocked in HPP and AAP nanoparticles, while in BAP nanoparticles, the net charge remained unaltered because the primary amino groups were converted into secondary ones.

3.5. Ethidium bromide exclusion assay

When HPP, AAP and BAP nanoparticles or PEI alone, were added to DNA:EtBr solution, the fluorescence intensity decreased (Fig. 4a–c). With a stepwise addition of heparin, a competitive anionic moiety, the fluorescence intensity increased progressively till it reached a plateau at 80% level with 25–30 units (Fig. 4a–c).

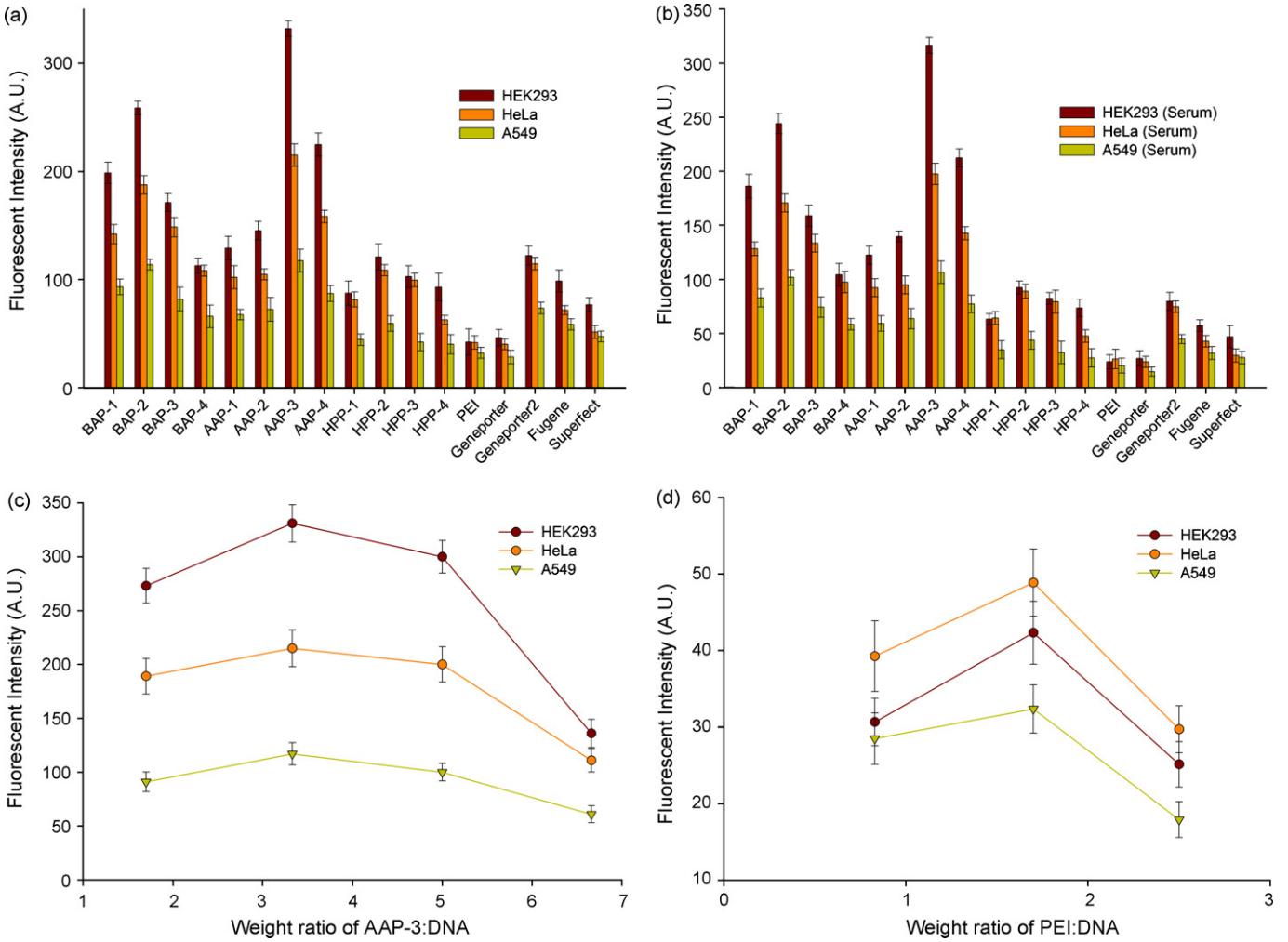

Fig. 5. GFP fluorescence intensity of (a) HEK293, HeLa and A549 cells; (b) HEK293, HeLa and A549 cells in presence of serum, transfected with HPP, AAP and BAP nanoparticle/DNA, PEI/DNA, GenePorter™/DNA, GenePorter2™/DNA, Superfect™/DNA and Fugene™/DNA complexes; (c) dose dependent GFP fluorescence intensity of AAP-3 nanoparticle/DNA complex; (d) dose dependent GFP fluorescent intensity of PEI/DNA complex in HEK293, HeLa and A549 cells. The transfection profiles show fluorescence intensity expressed in terms of arbitrary units/mg of total cellular protein obtained at a w:w ratio 3.33 for HPP, AAP and BAP nanoparticle/DNA complexes and 1.7 of PEI/DNA. Cells were incubated with the complexes for 4 h and the expression of GFP was monitored after 36 h. The fluorescent intensity of GFP fluorophore in the cell lysate was measured on spectrofluorometer. The results represent the mean of three independent experiments performed in triplicates.

Furthermore, the amount of heparin needed to release DNA from PEI/DNA complex was greater than that for nanoparticle/DNA complexes (Fig. 4a–c). Thus, the interaction of PEI with DNA is stronger than that of nanoparticles.

In contrast to the charge availability and open structure of PEI to bind DNA, a certain amount of the charge is embedded inside the core of the nanoparticles and may not be available for interaction. Among three nanoparticle series, the fluorescent intensity curves of AAP and BAP nanoparticle series are very similar, whereas, there is a significant difference in the fluorescent intensity curves of HPP nanoparticle series (Fig. 4). These results suggest that the dependency of degree of crosslinking on the extent of DNA binding to AAP and BAP nanoparticles is much less significant to that in HPP series, probably because the former two have more rigid structure due to covalent crosslinking unlike ionically crosslinked HPP nanoparticles that form relatively loose complex with DNA with lesser degree of DNA condensation, causing easier displacement of DNA by heparin with increased degree of crosslinking.

3.6. *In vitro cell transfection studies*

The *in vitro* transfection efficiency of HPP, AAP and BAP nanoparticles complexed with pGFP was compared with PEI and the commercial reagents such as GenePorter™, GenePorter2™, Superfect™ and Fugene™ in HeLa, HEK293 and A549 cells, in the presence and absence of serum. The study was carried out at w:w ratios higher than that required for complete DNA retardation. After 36 h of transfection, cells showed fairly high level of GFP gene expression (Fig. 5a–d) that was also quantified spectrofluorometrically and we found that the transfection efficiency first increased with increasing w:w ratio and then decreased beyond an optimal value (Fig. 5c and d). Among all nanoparticles, the highest level of gene expression was observed with AAP-3, followed closely by BAP-2 nanoparticles. AAP-3/DNA complex enhanced the gene transfer efficacy 2.7–7.8 folds as compared to PEI (25 kDa, gold standard) and commercially available transfecting reagents in HEK293 cells (Fig. 5a). As compared to native PEI, the transfection efficiency of AAP-3/DNA complex was 3.6 and 5.1 folds in A549 and HeLa cells, respectively. We observed that the transfection efficiency followed the trend AAP > BAP > HPP in all cell lines.

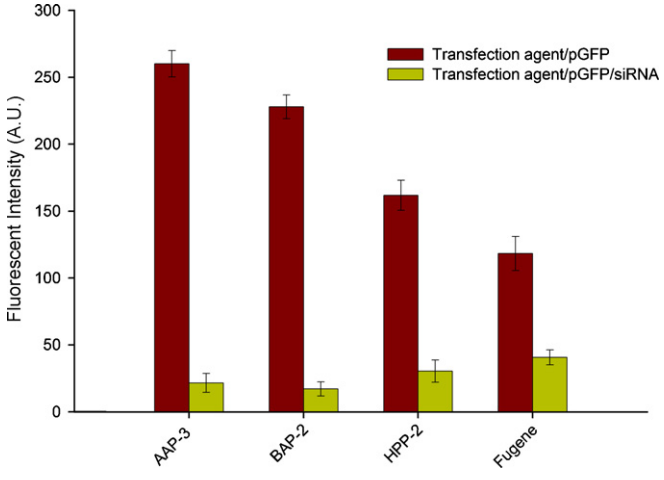

Fig. 6. AAP-3, BAP-2 and HPP-2 nanoparticles were checked for their ability to deliver siRNA in HeLa cells by transfecting pGFP DNA along with GFP-specific siRNA. The expression of GFP in cells was reduced by more than 81–92%, in comparison to Fugene™/pGFP/DNA/siRNA, which suppressed GFP expression by 65% only, as monitored by measuring fluorescence on a spectrofluorometer. All the experiments were performed at least thrice and error bars represent the standard deviation.

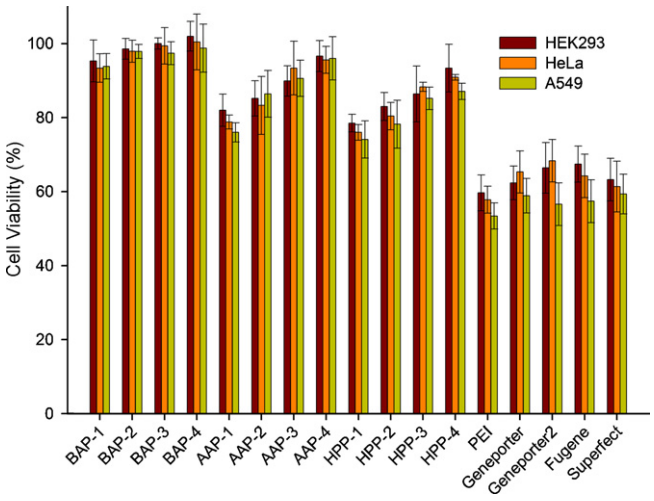

Fig. 7. Cell viability profile of HPP, AAP and BAP nanoparticle/DNA complexes (w:w ratio of 3.33) and PEI/DNA (w:w ratio of 1.7) in HEK293, HeLa and A549 cells, in comparison with GenePorter™/DNA, GenePorter2™/DNA, Superfect™/DNA and Fugene™/DNA complexes. Cells were treated with DNA complexes under conditions described in transfection, and cytotoxicity was determined by MTT assay. Percent viability of cells is expressed relative to control cells. Each point represents the mean of three independent experiments performed in triplicates.

The higher transfection efficiency HPP, AAP and BPP nanoparticles may also be due to hydrophobicity imparted to the system by the C-6 crosslinkers (SanJuan et al., 2007), leading to an enhanced gene expression. The type of crosslinking, degree of crosslinking and the w:w ratio of PEI/DNA complexes also appeared as important parameters for the enhanced transfection efficiency in the present study.

When transfection experiments were conducted in the presence of 10% serum, we found that the serum did not affect the release of DNA from the complexes and the resulting transfection efficiency of the three series of nanoparticle/DNA complexes (Fig. 5b). This speaks well for the practical utility of the nanoparticles for *in vivo* gene delivery.

3.7. *Delivery of siRNA using PEI nanoparticles*

The ability and efficiency of the nanoparticles to deliver siRNA along with pGFPDNA were compared with Fugene™ in HeLa cells. After 36 h of treatment, we observed suppression of GFP expression by HPP-2 (81%), AAP-3 (91%) and BAP-2 (92%) nanoparticle/DNA/siRNA complex (Fig. 6). In contrast, Fugene™/DNA/siRNA suppressed GFP expression only by 65% (Fig. 6). Thus GFP-specific siRNA oligonucleotides delivered by selected nanoparticles clearly down-regulated GFP gene more efficiently than Fugene™.

Table 3
IC_{50} value for PEI and crosslinked PEI nanoparticles (HPP, AAP and BAP) in HEK293 cells.

S. no.	Samples	IC_{50}
1	AAP-1	15
2	AAP-2	15
3	AAP-3	15
4	AAP-4	30
5	BAP-1	60
6	BAP-2	60
7	BAP-3	60
8	BAP-4	60
9	HPP-1	15
10	HPP-2	30
11	HPP-3	30
12	HPP-4	60
13	PEI	7.5

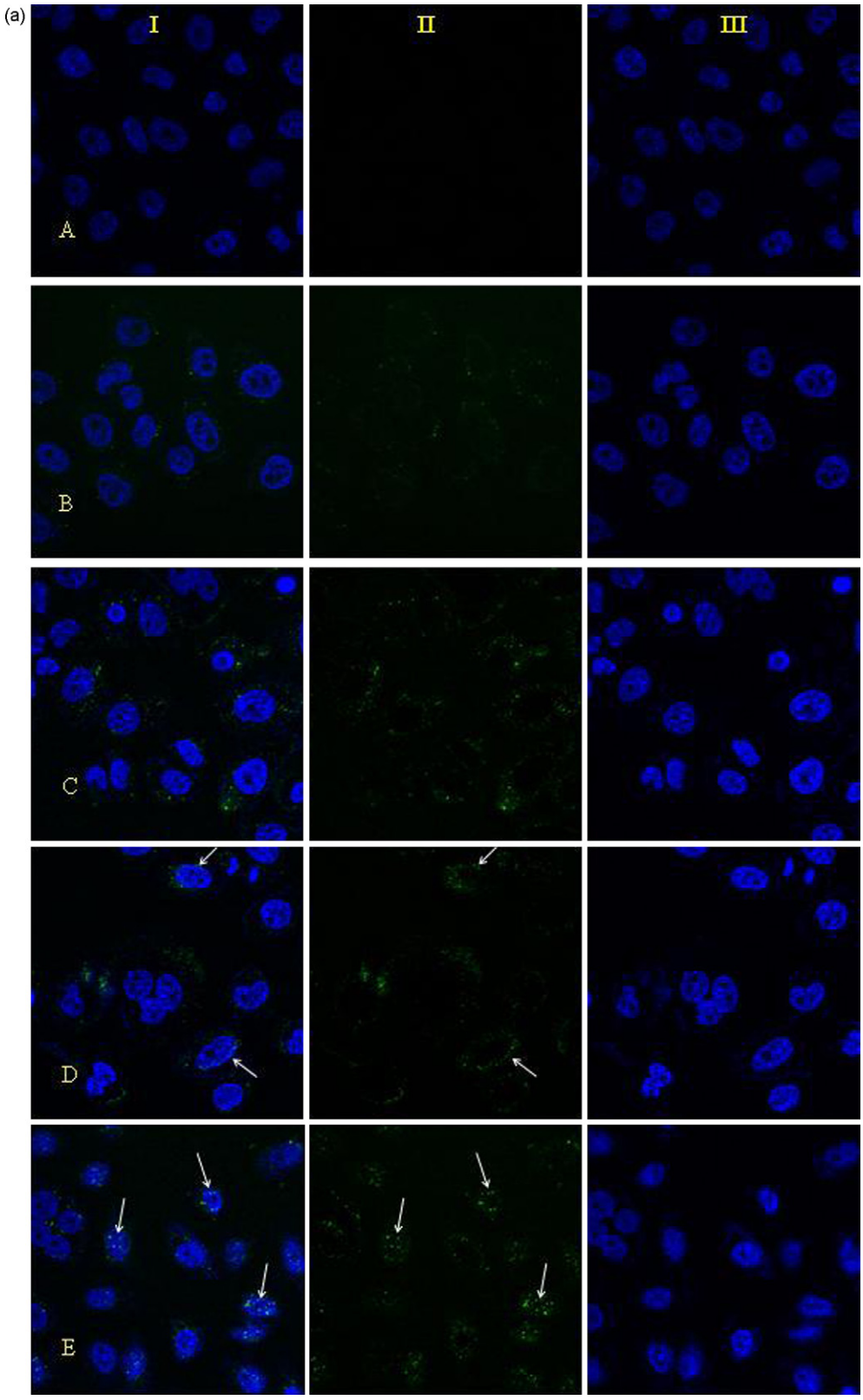

Fig. 8. Confocal microscopic images of HeLa cells treated with labeled AAP-3, BAP-2 and HPP-2 nanoparticles at different time points. (A) Control and fluorescein-labeled HPP-2 nanoparticle at (B) 30 min, (C) 1 h, (D) 2 h, (E) 4 h; fluorescein-labeled AAP-3 nanoparticle at (F) 30 min, (G) 1 h, (H) 2 h, (I) 4 h; fluorescein-labeled BAP-2 nanoparticle at (J) 30 min, (K) 1 h, (L) 2 h, (M) 4 h. The first quadrant (I) in each image represents the overlayed images, the second quadrant (II) represents images captured under fluorescein filter and the third quadrant (III) shows images captured under DAPI filter.

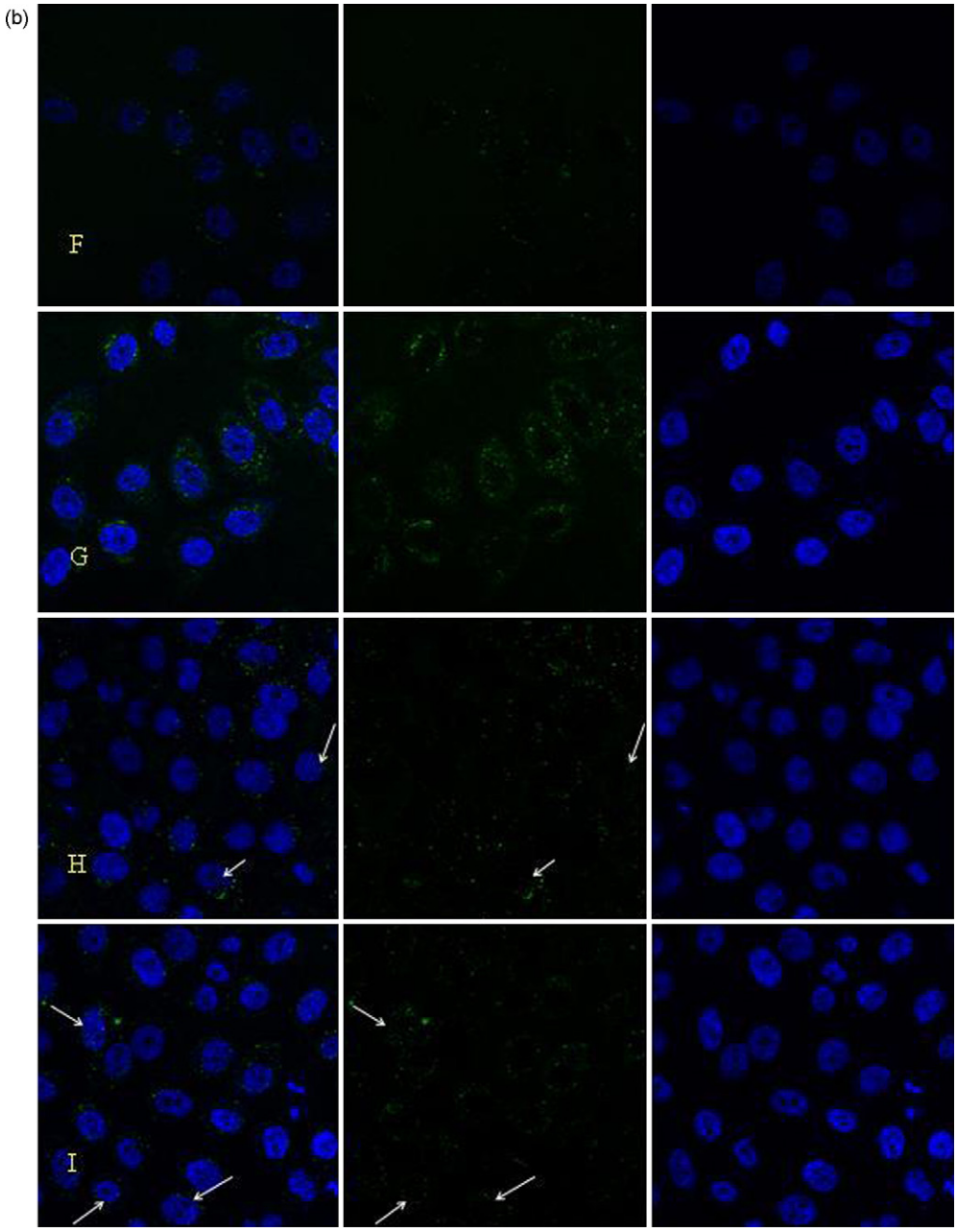

Fig. 8. (*Continued*)

3.8. Cell metabolic activity assay

Cytotoxicity is of the foremost concern for novel gene delivery systems. For example, PEI-based complexes transfect efficiently, but do confer significant cytotoxicity (Fischer et al., 2003; Jeong et al., 2006). In the present study, we evaluated the *in vitro* cytotoxicity of HPP, AAP and BAP nanoparticles in HEK293, HeLa and A549 cells, using MTT assay. PEI was considerably toxic (58% at a PEI/DNA w:w ratio 1.7). In contrast, PEI nanoparticles (HPP, AAP and BAP) exhibited no significant cytotoxicity and retained >85% cell viability (Fig. 7). For the three series of nanoparticles, BAP was least cytotoxic (5–10%), followed by AAP and HPP, in that order (Fig. 7). This is probably because of the conversion of the primary amino groups into secondary amino groups in BAP nanoparticles, which must have facilitated the escape of nanoparticle/DNA complexes from endosome (Gao and Liu, 2005). Other two series of nanoparticles, AAP and HPP showed increasing cell viability to 95% (AAP-4 and HPP-4) with increasing degree of crosslinking, as cytotoxicity was reduced through charge masking. A dose-dependent cytotoxicity was also observed with increasing concentration of PEI and PEI nanoparticles (data not shown). The IC_{50} values show that, compared to the nanoparticles, PEI remains highly toxic (Table 3).

3.9. Confocal laser scanning microscopy

Intracellular path of nanoparticles (HPP-2, AAP-3, BAP-2) was assessed by fluoresceinylating them with FITC such that 1% of amines on the nanoparticles were conjugated, which on analysis by TNBS assay revealed that only 0.28–0.35% of amines were modified and the zeta potential insignificantly decreased from 31.1 ± 1.4 to 30.7 ± 1.1 for HPP-2, 29.1 ±1.5 to 28.0 ±1.4 for AAP-3 nanoparticles and 33.8 ± 1.5 to 33.1 ±1.2 for BAP-2 nanoparticle formulation.

These labeled nanoparticles (AAP-3, BAP-2, HPP-2) were administered to HeLa cells and after 30 min, faint fluorescence appeared

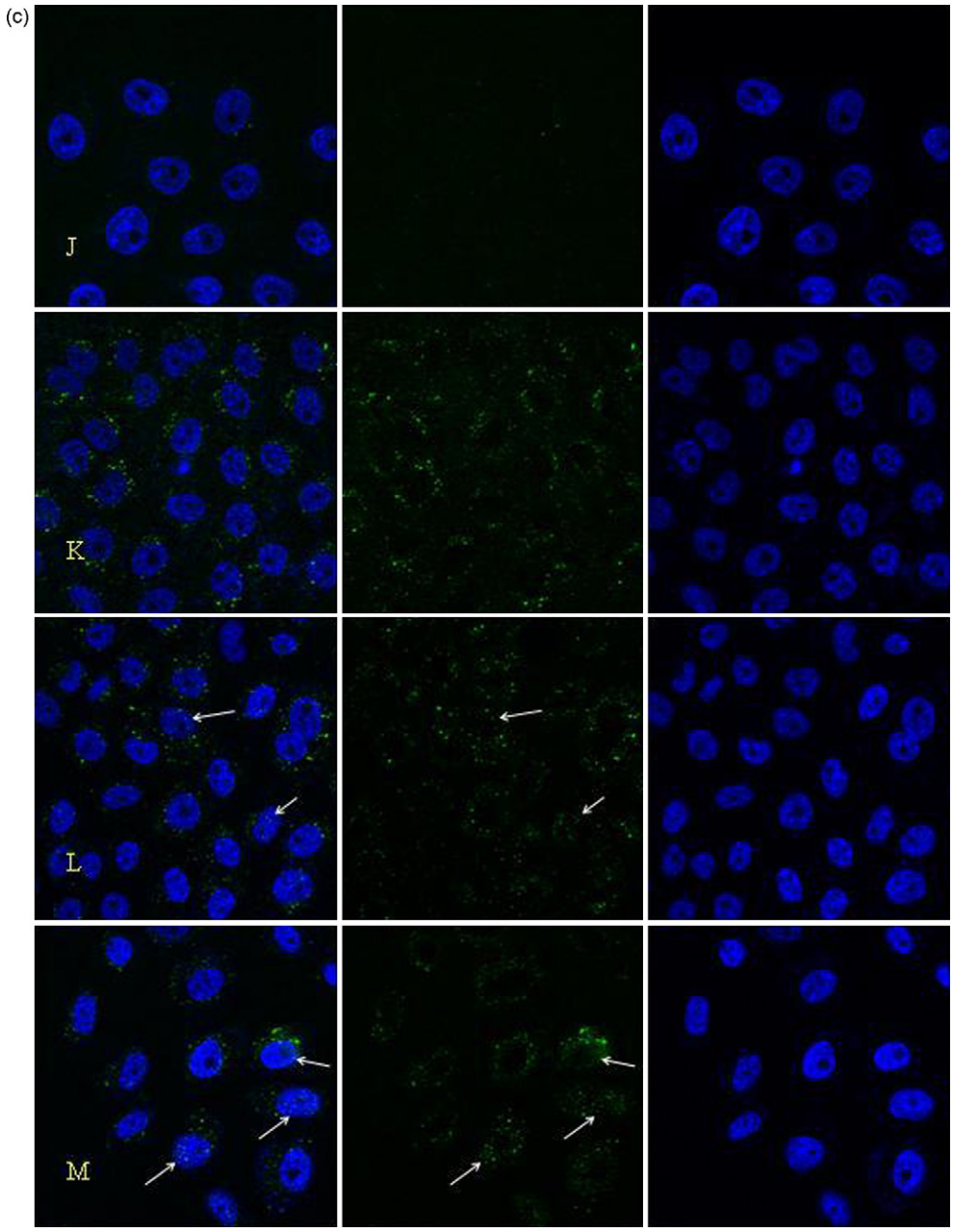

Fig. 8. (*Continued*).

around the plasma membrane, which moved well inside the cytoplasm after 1 h (Fig. 8). Subsequently, at 2–4 h, fluorescent particles became increasingly localized to the nuclei (Fig. 8). The observed nuclear localization of PEI nanoparticles is consistent with the work (Godbey et al., 1999) that showed labeled PEI is transported into cell nuclei. The time of entry of all labeled nanoparticles was nearly the same.

3.10. DNase I protection assay

In order to be an efficient gene delivery system, it should be able to confer protection to the complexed nucleic acids from degradation against nucleases present in the cellular environment. In DNase protection assay, we examined the ability of heparin to liberate intact DNA from DNase I treated nanoparticles/DNA complexes.

The ability of selected PEI nanoparticle (BAP-2) to shield DNA against DNase I was examined for different times and we found that in contrast to the free DNA (0.3 μg), which was degraded completely by DNase I in 15 min, BAP-2 nanoparticles effectively protected nanoparticle-bound DNA (Fig. 9) and provided protection to 88% after 30 min and 82% after 2 h. Thus, BAP-2 nanoparticles protected DNA against DNase I for a considerable time period and that the designed nanoparticles are suitable for *in vivo* administration of pDNA.

3.11. Body distribution

As BAP-2/DNA exhibited high transfection efficiency (Fig. 5) and negligible cytotoxicity (Fig. 7), we examined the time-dependent change in the distribution of intravenously injected ^{99m}Tc-labeled BAP-2/DNA complexes in the liver, kidney, spleen, lungs, stomach, intestine, heart, blood and brain of Balb/C mice. We found that the proportion of radioactive complex was highest in the liver (Fig. 10), which, after 1 h of injection, was 34.2 ± 1.8% ID declining

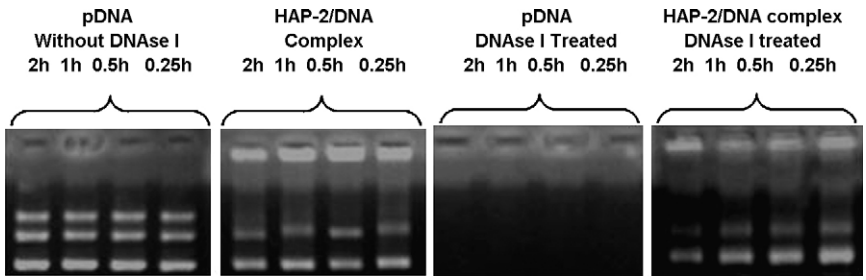

Fig. 9. DNaseI protection assay. Nanoparticle/DNA complex (BAP-2) was treated with DNase I (w:w ratio 3.33) for different time intervals. The complexed DNA was released by treating the samples with heparin. The amount of DNA protected (%) after DNase treatment is calculated as the relative integrated densitometry values (IDV) quantified and normalized by that of pDNA values (untreated with DNase I) using AlphaEaseFC software.

to 20.0 ± 1.7% ID after 24 h (Fig. 10). In comparison, the values for kidney were 0.92 ± 0.3% ID after 1 h declining to 0.5 ± 0.31% ID after 24 h (Fig. 10). Similar effect is observed for the heart, stomach, intestine and brain.

When radiolabeled BAP-2/DNA complex is injected in mice (Fig. 10) the complex is retained for at least 24 h *in vivo* and shows a differential distribution. The amount of labeled complex retained 6 h after injection was the highest (29.0 ± 1.9) in liver, which is understandable as blood is first diverted via portal vein to the liver, the centre for detoxification. This is in contrast to other organs. The overall body distribution pattern indicates that the BAP-2/DNA complexes are retained in the body for a significant time (Fig. 10) that may be useful for tissue-specific targeting of nanoparticles.

In conclusion, PEI nanoparticles (HPP, AAP and BAP), prepared using homobifunctional crosslinkers with fixed linker length and different functionalities, viz., phosphate, carboxyl and aldehydic groups, transfected various cell lines with high efficiency as compared to standard transfection reagents, showed no significant cytotoxicity. Among three series of nanoparticles, the highest transfection efficiency and cell viability were scored by AAP and BAP nanoparticles, respectively. Transfection with nanoparticle/DNA/siRNA suppressed the GFP expression by 80–90% in HeLa cells confirming the efficacy of the transfectants in delivering the specific gene and its inhibitors. Balb/C mice, receiving BAP-2/DNA complex, exhibit a differential accumulation in organs, highest being in the liver. Long retention time of these nanoparticles *in vivo* will be an asset in targeted gene/drug delivery.

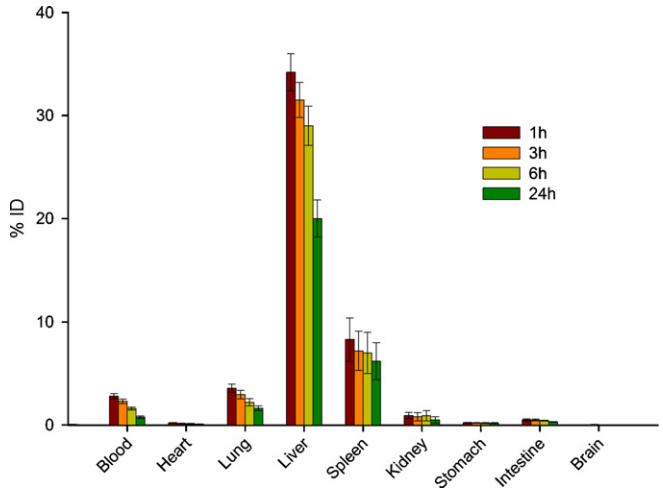

Fig. 10. Biodistribution pattern of radiolabeled BAP-2 nanoparticle/DNA complex.

Acknowledgments

Financial grants from the Department of Biotechnology and University Grant Commission, New Delhi, India, are gratefully acknowledged. Authors are thankful to Prof. S.P. Modak for his valuable scientific inputs during the preparation of this MS, Dr. Munia Ganguli for the help in AFM analysis, respectively.

References

Akinc, A., Thomas, M., Klibanov, A.M., Langer, R., 2005. Exploring polyethylenimine-mediated DNA transfection and the proton sponge hypothesis. J. Gene Med. 7, 657–663.
Banerjee, T., Singh, A.K., Sharma, R.K., Maitra, A.N., 2005. Labeling efficiency and biodistribution of Technetium-99m labeled nanoparticles: interference by colloidal tin oxide particles. Int. J. Pharm. 289, 189–195.
Davis, S.S., 1997. Biomedical applications of nanotechnology—implications for drug targeting and gene therapy. Trends Biotechnol. 15, 217–224.
Diebold, S.S., Kursa, M., Wagner, E., Cotten, M., Zenke, M., 1999. Mannose polyethylenimine conjugates for targeted DNA delivery into dendritic cells. J. Biol. Chem. 274, 19087–19094.
Edelstein, Michael L., 2007. Gene therapy clinical trials worldwide to 2007—an update. J. Gene Med. 9, 833–842.
Fischer, D., Li, Y., Ahlemeyer, B., Krieglstein, J., Kissel, T., 2003. In vitro cytotoxicity testing of polycations: influence of polymer structure on cell viability and hemolysis. Biomaterials 24, 1121–1131.
Gao, X., Liu, D., 2005. Selective chemical modification on polyethylenimine and its effects on transfection efficiency and cytotoxicity. Mol. Ther. 11, S427–S428.
Garg, M., Garg, B.R., Jain, S., Mishra, P., Sharma, R.K., Mishra, A.K., Dutta, T., Jain, N.K., 2008. Radiolabeling, pharmacoscintigraphic evaluation and antiretroviral efficacy of stavudine loaded 99mTc labeled galactosylated liposomes. Eur. J. Pharm. Sci. 33, 271–281.
Gebhart, C.L., Sriadibhatla, S., Vinogradov, S., Lemieux, P., Alakhov, V., Kabanov, A.V., 2002. Design and formulation of polyplexes based on pluronic–polyethyleneimine conjugates for gene transfer. Bioconjug. Chem. 13, 937–944.
Godbey, W.T., Wu, K.K., Mikos, A.G., 1999. Tracking the intracellular path of poly(ethylenimine)/DNA complexes for gene delivery. Proc. Natl. Acad. Sci. 96, 5177–5181.
Gosselin, M.A., Guo, W., Lee, R.J., 2001. Efficient gene transfer using reversibly cross-linked low molecular weight polyethylenimine. Bioconjug. Chem. 12, 989–994.
Guang Liu, W., De Yao, K., 2002. Chitosan and its derivatives—a promising non-viral vector for gene transfection. J. Control. Release 83, 1–11.
Hong, S., Leroueil, P.R., Janus, E.K., Peters, J.L., Kober, M.M., Islam, M.T., Orr, B.G., Baker, J.R., BanaszakHoll, M.M., 2006. Interaction of polycationic polymers with supported lipid bilayers and cells: nanoscale hole formation and enhanced membrane permeability. Bioconjug. Chem. 17, 728–734.
Itaka, K., Yamauchi, K., Harada, A., Nakamura, K., Kawaguchi, H., Kataoka, K., 2003. Polyion complex micelles from plasmid DNA and poly(ethylene glycol)-poly(-lysine) block copolymer as serum-tolerable polyplex system: physicochemical properties of micelles relevant to gene transfection efficiency. Biomaterials 24, 4495–4506.
Jeong, S.J., So, Y.K., Sang, B.L., Kyung, O.K., Joong, S.H., Young, M.L., 2006. Poly(ethylene glycol)/poly([epsilon]-caprolactone) diblock copolymeric nanoparticles for non-viral gene delivery: the role of charge group and molecular weight in particle formation, cytotoxicity and transfection. J. Control. Release 113, 173–182.
Kono, K., Akiyama, H., Takahashi, T., Takagishi, T., Harada, A., 2005. Transfection activity of polyamidoamine dendrimers having hydrophobic amino acid residues in the periphery. Bioconjug. Chem. 16, 208–214.
Malek, A., Czubayko, F., Aigner, A., 2008. PEG grafting of polyethylenimine (PEI) exerts different effects on DNA transfection and siRNA-induced gene targeting efficacy. J. Drug Target 16, 124–139.

Milligan, J.F., Uhlenbeck, O.C., 1989. In: James, E., Dahlberg, John, J. (Eds.), Synthesis of Small RNAs Using T7 RNA Polymerase. Academic Press, pp. 51–62.
More, J.D., Finney, N.S., 2002. A simple and advantageous protocol for the oxidation of alcohols WITH iodoxybenzoic acid (IBX). Org. Lett. 4, 3001–3003.
Nienhuis, A.W., 2008. Development of gene therapy for blood disorders. Blood 111, 4431–4444.
Niidome, T., Huang, L., 2002. Gene therapy progress and prospects: nonviral vectors. Gene Ther. 9, 1647–1652.
Nimesh, S., Aggarwal, A., Kumar, P., Singh, Y., Gupta, K.C., Chandra, R., 2007. Influence of acyl chain length on transfection mediated by acylated PEI nanoparticles. Int. J. Pharm. 337, 265–274.
Nimesh, S., Goyal, A., Pawar, V., Jayaraman, S., Kumar, P., Chandra, R., Singh, Y., Gupta, K.C., 2006a. Polyethylenimine nanoparticles as efficient transfecting agents for mammalian cells. J. Control. Release 110, 457–468.
Nimesh, S., Manchanda, R., Kumar, R., Saxena, A., Chaudhary, P., Yadav, V., Mozumdar, S., Chandra, R., 2006b. Preparation, characterization and in vitro drug release studies of novel polymeric nanoparticles. Int. J. Pharm. 323, 146–152.
Olefsky, J.M., 2000. Diabetes. Gene therapy for rats and mice. Nature 408, 420–421.
Pathak, A., Aggarwal, A., Kurupati, R., Patnaik, S., Swami, A., Singh, Y., Kumar, P., Vyas, S., Gupta, K., 2007. Engineered polyallylamine nanoparticles for efficient in vitro transfection. Pharm. Res. 24, 1427–1440.
Patnaik, S., Aggarwal, A., Nimesh, S., Goel, A., Ganguli, M., Saini, N., Singh, Y., Gupta, K.C., 2006. PEI-alginate nanocomposites as efficient in vitro gene transfection agents. J. Control. Release 114, 398–409.
Petersen, H., Fechner, P.M., Martin, A.L., Kunath, K., Stolnik, S., Roberts, C.J., Fischer, D., Davies, M.C., Kissel, T., 2002. Polyethylenimine-graft-poly(ethylene glycol) copolymers: influence of copolymer block structure on DNA complexation and biological activities as gene delivery system. Bioconjug. Chem. 13, 845–854.
Pirollo, K.F., Chang, E.H., 2008. Targeted delivery of small interfering RNA: approaching effective cancer therapies. Cancer Res. 68, 1247–1250.
Reddy, L.H., Sharma, R.K., Chuttani, K., Mishra, A.K., Murthy, R.R., 2004a. Etoposide-incorporated tripalmitin nanoparticles with different surface charge: formulation, characterization, radiolabeling, and biodistribution studies. AAPS J. 6, e23.
Reddy, L.H., Sharma, R.K., Murthy, R.S., 2004b. Enhanced tumour uptake of doxorubicin loaded poly(butyl cyanoacrylate) nanoparticles in mice bearing Dalton's lymphoma tumour. J. Drug Target 12, 443–451.
Reddy, L.H., Sharma, R.K., Chuttani, K., Mishra, A.K., Murthy, R.S., 2005. Influence of administration route on tumor uptake and biodistribution of etoposide loaded solid lipid nanoparticles in Dalton's lymphoma tumor bearing mice. J. Control. Release 105, 185–198.
Rosenecker, J., Huth, S., Rudolph, C., 2006. Gene therapy for cystic fibrosis lung disease: current status and future perspectives. Curr. Opin. Mol. Ther. 8, 439–445.
SanJuan, A., Letourneur, D., Izumrudov, V.A., 2007. Quaternized poly(4-vinylpyridine)s as model gene delivery polycations: structure–function study by modification of side chain hydrophobicity and degree of alkylation. Bioconjug. Chem. 18, 922–928.
Schmidt-Wolf, G.D., Schmidt-Wolf, I.G.H., 2003. Non-viral and hybrid vectors in human gene therapy: an update. Trends Mol. Med. 9, 67–72.
Seth, P., 2008. Gene therapy for cancer. JAMA 299, 1367–2136.
Sonawane, N.D., Szoka Jr., F.C., Verkman, A.S., 2003. Chloride accumulation and swelling in endosomes enhances DNA transfer by polyamine-DNA polyplexes. J. Biol. Chem. 278, 44826–44831.
Swami, A., Kurupati, R.K., Pathak, A., Singh, Y., Kumar, P., Gupta, K.C., 2007a. A unique and highly efficient non-viral DNA/siRNA delivery system based on PEI-bisepoxide nanoparticles. Biochem. Biophys. Res. Commun. 362, 835–841.
Swami, A., Aggarwal, A., Pathak, A., Patnaik, S., Kumar, P., Singh, Y., Gupta, K.C., 2007b. Imidazolyl-PEI modified nanoparticles for enhanced gene delivery. Int. J. Pharm. 335, 180–192.
Tabatt, K., Kneuer, C., Sameti, M., Olbrich, C., Muller, R.H., Lehr, C.M., Bakowsky, U., 2004. Transfection with different colloidal systems: comparison of solid lipid nanoparticles and liposomes. J. Control. Release 97, 321–332.
Thakkar, H., Sharma, R.K., Mishra, A.K., Chuttani, K., Murthy, R.S., 2004. Efficacy of chitosan microspheres for controlled intra-articular delivery of celecoxib in inflamed joints. J. Pharm. Pharmacol. 56, 1091–1099.
Tseng, W.C., Tang, C.H., Fang, T.Y., 2004. The role of dextran conjugation in transfection mediated by dextran-grafted polyethylenimine. J. Gene Med. 6, 895–905, Ref. type: Generic.
Vinge, L.E., Raake, P.W., Koch, W.J., 2008. Gene therapy in heart failure. Circ. Res. 102, 1458–1470.
Walker, G.F., Fella, C., Pelisek, J., Fahrmeir, J., Boeckle, S., Ogris, M., Wagner, E., 2005. Toward synthetic viruses: endosomal pH-triggered deshielding of targeted polyplexes greatly enhances gene transfer in vitro and in vivo. Mol. Ther. 11, 418–425.
Zhang, X., Godbey, W.T., 2006. Viral vectors for gene delivery in tissue engineering. Adv. Drug Deliv. Rev. 58, 515–534.